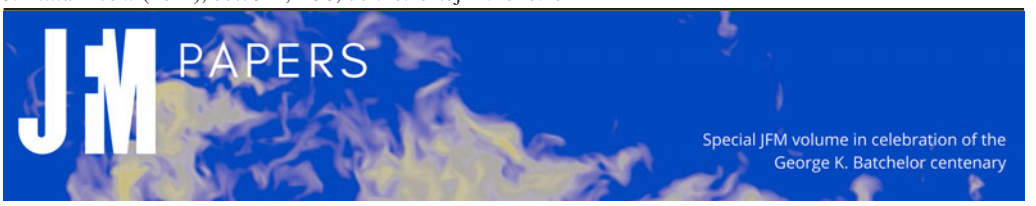
CrossMark

J. Fluid Mech. (2021), *vol*. 914, A38, doi:10.1017/jfm.2020.1022



Physics of road cycling and the three jerseys problem*

Caroline Cohen[1], **Emmanuel Brunet**[2], **Jérémy Roy**[2] **and Christophe Clanet**[1],†

[1]LadHyX, UMR 7646 du CNRS, Ecole Polytechnique, 91128 Palaiseau, France

[2]Fédération Française de Cyclisme, 1 rue Laurent Fignon, 78180 Montigny-Le-Bretonneux, France

(Received 5 April 2020; revised 14 September 2020; accepted 10 November 2020)

Tour de France, Giro d'Italia and Vuelta a España in Spain are the three grand tours of professional road cycling. Three weeks long with daily stages, these three races all use three jerseys to distinguish the leader, the best sprinter and the best climber. We first discuss the physics of road cycling and show that these three jerseys are associated with three different dynamical regimes. We then propose a phase diagram for road cycling which enables us to discuss the different physiological characteristics observed in the peloton. We finally establish the phase diagram for the Tour de France 2017 and show that the final three jerseys do belong to the expected three optimal regions of the phase diagram.

Key words: aerodynamics

1. Introduction

The science of cycling is the subject of many studies reported in books (Wilson & Schmidt 2020) and reviews (Faria, Parker & Faria 2005*a*,*b*; Crouch *et al.* 2017). Here, we focus on the specific question of the different dynamics observed in road cycling during professional grand tours and their impact on the rewards used (jerseys).

The oldest grand tour is the Tour de France (1903) which was initially 2428 km long in six stages, organized by the newspaper 'L'Auto' and inspired by the popular six days on track races (Chany 1983; Lucia, Earnest & Arribas 2003; Mignot 2016). The Giro d'Italia and the Vuelta a España started in 1909 (2448 km) and in 1935 (3425 km), respectively, and were also organized by newspapers, 'La Gazzetta dello Sport' and 'Informaciones'. Since 1919, the leader of the general classification wears the yellow jersey in the Tour

† Email address for correspondence: clanet@ladhyx.polytechnique.fr
A video presentation about this research work can be found at:
https://www.cambridge.org/clanet-abstract.
*Graphical Abstract image reproduced with permission from George Batchelor's daughters: Adrienne and Bryony

© The Author(s), 2021. Published by Cambridge University Press

https://doi.org/10.1017/jfm.2020.1022 Published online by Cambridge University Press

(introduced by Henri Desgrange) and the pink jersey in the Giro since 1931. These colours being those of the newspapers L'Auto and La Gazzetta dello Sport. The history for the Vuelta is more complex: the jersey has been orange (1935, 1942, 1977), white (1941), white with a red stripe (1945–1950), yellow (1955–1976, 1978–1997), gold (1998–2009) and finally red since 2010.

Besides the general classification, grand tours also reward the best climber via the classification of the king-of-the-mountains (Tour and Giro since 1933, Vuelta since 1935) and the best sprinter by points classification (Vuelta since 1945, Tour since 1953 and Giro since 1966) (Mignot 2016). The point classification rewards the rider who has accumulated the most points over all the stages. The greatest number of points being awarded to the first place of each stage; however, the scale is not fixed and a greater number of points is awarded for the so-called plain stages intended for sprinters. An intermediate sprint during the stage also allows you to collect points. For these reasons, most of the time the point jersey goes to a sprinter.

All the jerseys were introduced after the first classifications and their colours have their own history: concerning the sprint, the green jersey in the Tour was first introduced in 1953 for the 50th anniversary. The colour green came from the sponsor 'la belle jardinière' (Soula 2013). The corresponding jerseys for the Vuelta and the Giro appeared in 1955 and 1967.

For the best climber in Tour de France, the polka-dot jersey was introduced in 1975 by Félix Lévitan, director of 'la Société du Tour de France', in memory of Henri Lemoine, the French track cyclist used these colours with his teammate Marcel Guimbretière (Carrey 2015). For the Giro, the jersey for the best climber was introduced in 1974 and was initially green (Carrey, Turgis & Endrizzi 2019). For the Vuelta, it appeared in 1976.

While the first few Tour de France were less than 3000 km long, they soon evolved to long editions (>5000 km) divided into 14 to 17 stages. This peaked in 1927 with 5745 km in 17 stages (∼337 km per stage) where each stage lasted typically ∼14 h, leading to the legend of 'convicts of the road'. High mountain stages were introduced in 1910 for the Pyrenees (Tourmalet and Aubisque) and in 1911 for the Alps (Galibier). The first time trial appeared in 1934. The current configuration is composed of 21 stages raced over three weeks. General information on the three grand tours in 2019 is summarized in figure 1. We observe that they have almost the same total distance of 3400 ± 150 km and are run with almost the same average speed of 39.9 ± 0.7 km h^{-1}.

The three grand tours have been the subject of a large number of studies and books (Chany 1983; Fallon & Bell 2005; McGann & McGann 2008, 2012; Carrey *et al.* 2019). Here, we only discuss the physics involved in road cycling and its impact on these stage races. The general features of grand tours are presented in § 2, the model in § 3 and its connection to the three jerseys is discussed via the phase diagram presented in § 4 prior to the conclusion.

2. General characteristics in road cycling grand tour

The range of velocities observed during Tour de France is presented in figure 2: unsurprisingly, the slowest velocity is measured in high mountain where the mean slope $\bar{\alpha}$ of the order of $+8\,\%$ is climbed with a characteristic velocity of 20 km h^{-1} (Vogt *et al.* 2008). At the opposite limit, one finds the descent where velocities as high as 100 km h^{-1} are regularly recorded (Blocken *et al.* 2018*a*).

In between these two limits we mention the characteristics of flat time trial, where the cyclists typically run one hour at 50 km h^{-1} (Earnest *et al.* 2009) and sprints which last

https://doi.org/10.1017/jfm.2020.1022 Published online by Cambridge University Press

2019	Leader	Climber	Sprinter (points)
3366 km Tour de France	Egan Bernal 22 y.o. 1.75 m 60 kg 40 576 km h^{-1}	Romain Bardet 29 y.o. 1.84 m 65 kg	Peter Sagan 29 y.o. 1.82 m 79 kg
Giro 3546.8 km	Richard Carapaz 26 y.o. 1.70 m 62 kg 39.41 km h^{-1}	Giulio Ciccone 24 y.o. 1.76 m 58 kg	Pascal Ackermann 25 y.o. 1.80 m 78 kg
Vuelta 3291 km	Primoz Roglic 30 y.o. 1.77 m 65 kg 39 587 km h^{-1}	Geoffrey Bouchard 27 y.o. 1.77 m 64 kg	Primoz Roglic 30 y.o. 1.77 m 65 kg

Figure 1. General information for the three grand tours in 2019: for the different jerseys, we indicate the name of the winner, his age, size and mass, as well as, for the leader, his average velocity.

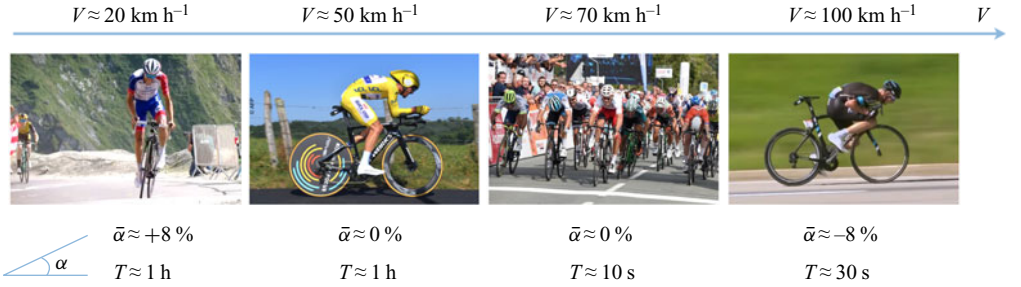


Figure 2. Range of velocities observed during Tour de France: α stands for the slope of the road, $\bar{\alpha}$ for its mean value and T for the typical duration of the climb, time trial (TT), sprint and descent (from left to right). Photo credits: T. Vergouwen/AFP/Presse Sport.

typically 10 s and where the athletes reach 70 km h^{-1} over a few seconds (Menaspa, Abbiss & Martin 2013; Blocken *et al.* 2019). Beyond these orders of magnitudes, the precise values of the velocities, slopes and durations for these different stages are presented in the following sections.

Throughout the article we use the classification of stages defined by race organizers (Padilla *et al.* 2001): flat stages (FLT), in which the total distance riding uphill is shorter that 13 km, the total altitude change is lower than 800 m and the hills are scattered along the stage, but never at the end of it; semi-mountainous stages (SMT), with a total uphill distance of between 13 and 35 km, and a total altitude change ranging between 800 and 2000 m; high-mountain stages (MT), in which the total uphill distance is longer than 35 km, and the total altitude change is higher than 2000 m. Stages finishing with more than 12 km uphill and an altitude change of more than 800 m are also included in this (MT) category.

https://doi.org/10.1017/jfm.2020.1022 Published online by Cambridge University Press

The anthropometric profiles of riders in the Tour (body mass M_c, height L_c and body-mass index BMI $= M_c/L_c^2$) have been studied and correlated to their success during the different types of stages (Lucia, Joyos & Chicharro 2000; Santalla *et al.* 2012): TT specialists are generally 180 to 185 cm tall, weigh 70 to 75 kg and have a BMI $\sim$ 22 kg m^{-2}. This anthropometry allows them to achieve higher absolute power outputs (W) than climbers (175–180 cm, 60–66 kg, BMI = 19–20 kg m^{-2}), who are better able to maintain a higher power to mass ratio (W kg^{-1}) (Padilla *et al.* 1999; Lucia *et al.* 2000).

3. Physics of road cycling

The problem of cycling is sketched in figure 3(*a*). The dynamics of the rider is governed by the balance of energy

$$\frac{\mathrm{d}}{\mathrm{d}t}\left(\frac{1}{2}MV^2 + Mgz\right) = P_m - P_f, \tag{3.1}$$

where V is the velocity of the centre of mass, z the vertical elevation, g gravity and M stands for the total mass, $M = M_c + M_b$ (M_c and M_b being respectively the mass of the cyclist and of the bike). At the moment the legal minimal mass for bikes on the Tour is 6.8 kg and the typical mass for bikes in TT is 8 kg. On the right-hand side of (3.1), P_m is the mechanical power injected by the cyclist and P_f is the power dissipated by friction (di Prampero *et al.* 1979).

Studies dedicated to the friction reveal that P_f is mainly composed of aerodynamic and rolling resistance $P_f = \frac{1}{2}\rho S C_D V^3 + \mu M g V$, where ρ is the density of air, S is the frontal area of the cyclist and bicycle which experience a drag coefficient C_D (here, the product SC_D will be referred to as the 'drag area') and μ is the rolling resistance coefficient (Martin *et al.* 1998; Crouch *et al.* 2017). Since the aerodynamic drag increases as V^3 and the rolling resistance as V, there is a velocity V_μ for which both contributions are equal: $V_\mu = \sqrt{2\mu Mg/\rho SC_D}$. Using typical values $\rho = 1.2$ kg m^{-3}, $SC_D = 0.25$ m^2, $\mu = 0.0032$ and $M = 80$ kg, we get $V_\mu \approx 15$ km h^{-1}. Since the velocities in Tour de France are larger than V_μ the main contribution will be aerodynamic and we will generally neglect rolling resistance in this study. The only exception will be in the section dedicated to climbing where the velocities get close to V_μ.

Concerning the maximal mechanical power produced by the cyclist, P_m, it depends on both the pedalling rate, $\dot{\theta}$, and the duration of the exercise, T. As shown by Dorel *et al.* (2005), the relation between the mechanical power and the pedalling rate is parabolic

$$P_m\left(\dot{\theta}, T\right) = 4P_{max}(T)\frac{\dot{\theta}}{\dot{\theta}_{max}}\left(1 - \frac{\dot{\theta}}{\dot{\theta}_{max}}\right), \tag{3.2}$$

where $\dot{\theta}$ is the pedalling rate, $\dot{\theta}_{max}$ its maximum value and $P_{max}(T)$ the maximum power which can be developed over the duration T. Two examples reproduced from Dorel *et al.* (2005) obtained with track cyclists with $T = 5$ s exercises are presented in figure 3(*b*). For the hollow circles, one reads $\dot{\theta}_{max} \approx 260$ r.p.m. and $P_{max} \approx 1800$ W. Since the power is maximal for a given pedalling rate, one expects professional road cyclists to ride at a fix pedalling rate and to use gears to adapt to the road profile. This is indeed what is reported in the literature: considering FLT, SMT and MT stages, Vogt *et al.* (2007) reports that the average cadense was 87, 86 and 81 r.p.m. respectively'.

https://doi.org/10.1017/jfm.2020.1022 Published online by Cambridge University Press

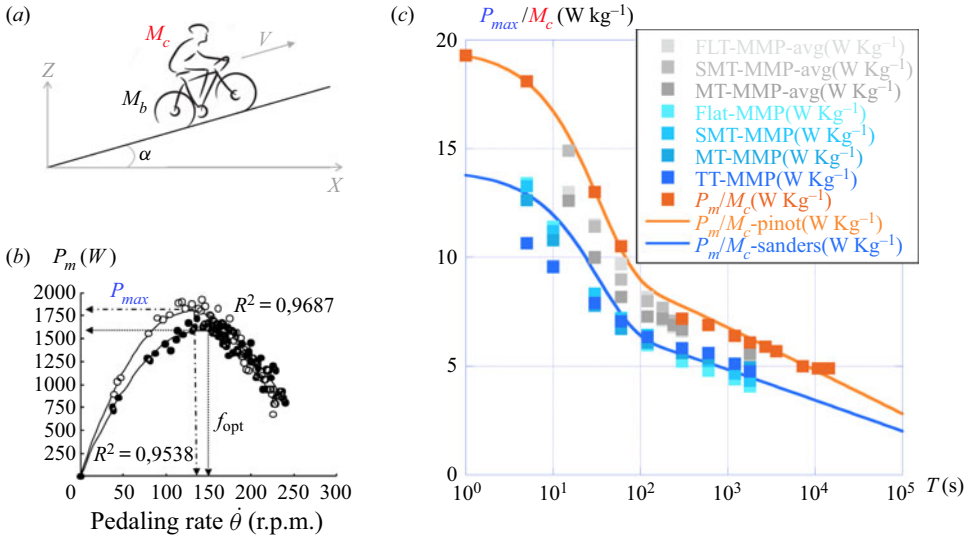


Figure 3. Elements for the model: (*a*) schematics of the cyclist of mass M_c and of his bike of mass M_b climbing a slope of angle α. (*b*) Evolution of the power, P_m, with the pedalling rate, $\dot{\theta}$, for two different athletes (reproduced from Dorel *et al.* (2005)). (*c*) Time evolution of the power to mass ratio, P_{max}/M_c, in cycling: the grey points are the maximal mean power (MMP) obtained for 15 riders of Tour de France 2005 ranking from 40 to 150 by Vogt *et al.* (2007). The different greys are used to differentiate road type (FLT, flat; SMT, semi-mountainous; MT, mountainous). The blue points are the MMP obtained for 9 riders from the same professional team on the Giro 2016 and reported by Sanders & Heijboer (2019). As for greys, the different blues are used to distinguish the different types of road. Plus dark blue for TT. The orange points corresponds to a single top 10 rider of the Tour de France studied by Pinot & Grappe (2014). The two solid lines correspond to the predictions of the heuristic equation (3.3) using $\tau = 32$ s, $\gamma = 0.0886$ and $\Pi = 9.7$ W kg^{-1} for the orange line and $\Pi = 7$ W kg^{-1} for the blue line.

The maximum power per unit of mass P_{max}/M_c is presented as a function of time T on a log–linear scale in figure 3(*c*): the three different sets of colours (grey, blue and orange) correspond to three different studies. The grey points have been obtained on Tour de France 2005 with 15 different riders ranking from 40 to 150 (Vogt *et al.* 2007). The blue set has been obtained with 9 riders of the same professional team on Giro 2016 (Sanders & Heijboer 2019). For each set, a different intensity is used to distinguish the different types of roads (FLT, SMT, MT). No big difference is observed between the different intensities. We will thus assume that P_{max}/M_c is independent of the road type. Finally, the orange points have been obtained for a single rider top 10 Tour de France finisher (Pinot & Grappe 2014).

The log–linear scale used in figure 3(*c*) reveals that the power to mass ratio reaches values of the order of 14–19 W kg^{-1} during very short periods (several seconds) and then decreases as the duration of the effort increases down to a quasi-plateau of the order of 5–6 W kg^{-1}, reached after few minutes. For the single rider (orange points) the power to mass ratio is 18.1 W kg^{-1} during 5 s, 7.2 W kg^{-1} after 5 min, 6.9 W kg^{-1} after 10 min, 5.7 W kg^{-1} after 1 h and 4.9 W kg^{-1} after 4 h.

The continuous lines presented in figure 3(*c*) correspond to the heuristic fit of the power to mass ratio

$$\frac{P_{max}(T)}{M_c} = \Pi[\mathrm{e}^{-T/\tau} + 1 - \gamma \ln(T/\tau + 1)]. \tag{3.3}$$

https://doi.org/10.1017/jfm.2020.1022 Published online by Cambridge University Press

For the two cases plotted in figure 3(*c*), $\tau = 32$ s, $\gamma = 0.0886$ and $\Pi = 9.7$ W kg^{-1} for the orange line and $\Pi = 7$ W kg^{-1} for the blue line. To discuss the records observed in Tour de France we will use the value obtained for the top 10 finisher ($\Pi = 9.7$ W kg^{-1}).

The physical interpretation of this heuristic fit is that the power to mass ratio reaches its maximal value at short times $\lim_{T/\tau \ll 1}(P_{max}/M_c) = 2\Pi$ and then decreases over a characteristic time τ of the order of 30 s to a quasi-plateau $\lim_{T/\tau \gg 1}(P_{max}/M_c) = \Pi[1 - \ln(T/\tau)^{\gamma}]$. These two regimes correspond to the anaerobic regime ($T < \tau$) and to the aerobic regime ($T \gg \tau$). The initial exponential decrease of the power has already been reported and modelled by Sanders & Heijboer (2018). In their study, they use a similar value for the characteristic time of the anaerobic phase ($\tau = 38.4$ s). The log term in the heuristic fit (3.3) describes the slow decrease of the power to mass ratio in the long efforts limit (Morton & Hodgson 1996). It accounts for the effect of fatigue: if $\gamma = 0$ there is no fatigue and if γ is positive ($\gamma > 0$), the larger its value the stronger the effect of fatigue. Figure 3(*c*) shows that the value $\gamma = 0.0886$ allows us to account for fatigue for the different sets of data taken from the literature.

This discussion on the different terms of (3.1) reveals that the term P_m is 'active' and depends on the skills of the cyclist while the three other terms are 'passive'. Equation (3.1) can thus be rewritten in order to show how the human power P_m is used:

$$P_m = \frac{1}{2}\rho S C_D V^3 + Mg\alpha V + \frac{\mathrm{d}}{\mathrm{d}t}\left(\frac{1}{2}MV^2\right). \tag{3.4}$$

Equation (3.4) thus reveals that human power can be stored in three different terms, the aerodynamic friction $\frac{1}{2}\rho S C_D V^3$, the ascending term $Mg\alpha V$ and the accelerating term $\mathrm{d}/\mathrm{d}t(MV^2/2)$. Each of these terms is connected to different cycling regimes which are discussed below.

3.1. *Time trial*

The results from all individual TTs in Tour de France from 2010 to 2019 are presented in table 1. For the winner, the average velocity $\bar{V}_{TT} = D/T$, defined as the ratio between the distance D of the TT and his time T, is indicated in column 9. Even if the distance of TT changes from 6.4 km to 54 km we observe that flat TTs (type FLT in blue) are covered with a mean velocity of the order of 52.5 ± 2.5 km h^{-1} while TTs in mountain regions (type MT in red) have velocities of the order of 35 ± 2 km h^{-1}. We first address the limit of flat TTs and treat the general case in a second step.

3.1.1. *Flat time trial*

Since TT is observed to be a steady effort ($\mathrm{d}/\mathrm{d}t = 0$), (3.4) states that, in the limit of FLT ($\alpha = 0$), the mechanical power is mainly injected in aerodynamical friction so that the equation for flat TT reduces to $P_m \approx 1/2\rho S C_D V^3$. To maximize his velocity the rider will select $P_m = P_{max}$ and for long time efforts ($T \gg \tau$), the power P_m will reach the quasi-plateau associated with aerobic efforts presented in figure 3(*c*). One thus deduces the characteristic velocity for flat TT

$$V_{TT}(T) = \left(\frac{2P_{max}(T)}{\rho S C_D}\right)^{1/3}. \tag{3.5}$$

Using $P_{max}(T) = \Pi M_c[1 - \ln(T/\tau)^{\gamma}]$ with $\Pi = 9.7$ W kg^{-1}, $\tau = 32$ and $\gamma = 0.0886$ we evaluate $P_{max}(T)$ for each rider in table 1 (column 10).

https://doi.org/10.1017/jfm.2020.1022 Published online by Cambridge University Press

Year	Stage	Type	Winner	L_c (m)	M_c (kg)	D (km)	T (h min s)	$\bar{V}_{TT}$ (km h^{-1})	$P_{max}(T)$ (W)	$V_{TT}(T)$ (km h^{-1})	Error (%)
2019	13	SMT	J. Alaphilippe	1.73	62	27.2	35′ 00″	46.6	378	48.9	5.0
2018	20	SMT	T. Dumoulin	1.85	69	31	40′ 52″	45.5	411	50.3	10.7
2017	1	FLT	G. Thomas	1.83	71	14	16′ 04″	52.3	479	53	1.4
	20	SMT	M. Bodnar	1.86	75	22.5	28′ 15″	47.8	470	52.7	10.2
2016	13	SMT	T. Dumoulin	1.85	69	37.5	50′ 15″	44.8	399	49.9	11.4
	18	MT	C. Froome	1.86	66	17	30′ 43″	33.2	409	50.3	51.5
2015	1	FLT	R. Dennis	1.82	72	13.8	14′ 56″	55.4	490	53.4	3.6
2014	20	SMT	T. Martin	1.85	75	54	1h 6′ 21″	48.8	416	50.5	3.6
2013	11	FLT	T. Martin	1.85	75	33	36′ 29″	54.3	454	52	4.0
	17	MT	C. Froome	1.86	66	33	51′ 33″	38.4	380	49.0	27
2012	1	FLT	F. Cancellara	1.86	82	6.4	7′ 13″	53.2	606	57.3	7.8
	9	SMT	B. Wiggins	1.90	69	41.5	51′ 24″	48.4	397	49.8	2.8
	19	FLT	B. Wiggins	1.90	69	53.5	1h 4′ 13″	50.0	384	49.3	1.4
2011	20	SMT	T. Martin	1.85	75	42.5	55′ 33″	45.9	427	51.0	11.1
2010	1	FLT	F. Cancellara	1.86	82	8.9	10′ 0″	53.4	585	56.6	6.1
	19	FLT	F. Cancellara	1.86	82	52	1h 0′ 56″	51.2	460	52.3	2.2

Table 1. Results from all individual TTs in Tour de France from 2010 to 2019. Flat TTs are indicated with (FLT), hilly time trials with (SMT) and those in mountains with (MT). The name of the winner is given together with his height L_c and mass M_c. The distance D of the TT is given together with the best time T. From these values, we calculate the actual average velocity $\bar{V}_{TT} = D/T$. The expected power is calculated using (3.3) with the time of the race T and the mass M_c of the winner. The predicted velocity $V_{TT}(T)$ is calculated using (3.5). The error between $\bar{V}_{TT}$ and $V_{TT}(T)$ is given in the last column.

Concerning the drag area, SC_D, recent experimental and numerical studies have revealed the complex structure of the flow around the cyclist (Crouch *et al.* 2014; Hosoi 2014). This complexity is illustrated in figure 4(*a*) using the isosurfaces of average streamwise vorticity (reproduced from Griffith *et al.* 2014). A summary of the values of SC_D found in wind tunnels and reported in the literature is presented in figure 4(*b*). For the TT position we observe that $SC_D \approx 0.25$ m^{-2}. Using $\rho = 1.2$ kg m^{-3} we calculate $V_{TT}(T)$ with (3.5) and evaluate the error with the actual value $\bar{V}_{TT}$ in the last column of table 1. For all flat TT (FLT in blue) we observe that the error is smaller than 8 %. For hilly (SMT) and mountain types (MT) the velocity V_{TT} predicted by assuming $\alpha = 0$ is unsurprisingly larger than the actual one and the discrepancy can reach 50 %.

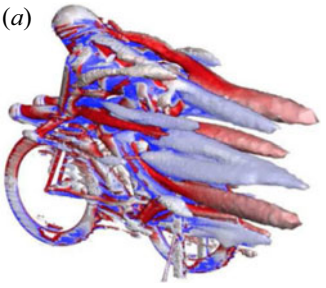
3.1.2. *Non-flat time trial*

While studying TT performance in § 3.1.1, we underlined that the velocity V_{TT} predicted by (3.5) only holds in the limit of a flat road ($\alpha = 0$). When this limit is not achieved, observations show that the average velocity is significantly reduced (table 1). For the case of the individual TT of the 18th stage of the Tour de France 2016, the road profile is clearly not flat, as illustrated in figure 5(*a*). As presented in table 1, Froome wins the stage with a mean velocity of 33.2 km h^{-1}, far below the 50 km/h predicted by (3.5) for the flat TT limit.

To account for gravity, one needs to reconsider the equation of motion (3.4) without the unsteady term (TT is a steady regime) but with the gravitational contribution: $P_m = 1/2\rho SC_D V^3 + Mg\alpha V$. Using the flat limit expression $V_{TT}(T) = (2P_{max}(T)/\rho SC_D)^{1/3}$,

https://doi.org/10.1017/jfm.2020.1022 Published online by Cambridge University Press

(*a*)



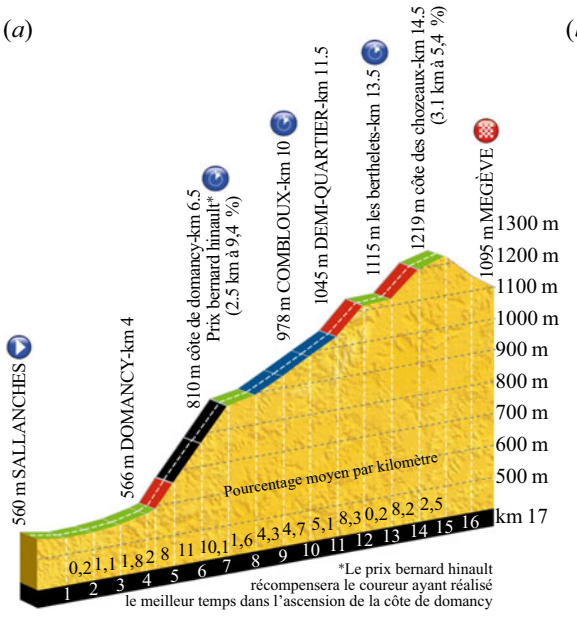
(*b*)



Study	Measurment	Upright	Dropped	Time-trial	Velocity (m s^{-1})
1	$S.C_D$ (m^2)		0.28		1.5-18.5
2	$S.C_D$ (m^2)	0.32	0.26		8.9-15.6
3	$S.C_D$ (m^2)			0.269	13.4
4	$S.C_D$ (m^2)			0.244	13.9
5	$S.C_D$ (m^2)	0.358	0.307	0.269-0.240	12.8
6	$S.C_D$ (m^2)			0.260	15
7	$S.C_D$ (m^2)	0.52-0.43		0.293-0.341	15
8	$S.C_D$ (m^2)	0.318-0.282	0.289-0.275	0.235-0.223	13.9
9	$S.C_D$ (m^2)			0.296-0.226	11.1
10	$S.C_D$ (m^2)	0.270	0.243	0.211	10-20
11	$S.C_D$ (m^2)	0.343	0.332-0.295		12.5
12	$S.C_D$ (m^2)			0.251-0.214	18

Figure 4. Isosurfaces of average streamwise vorticity behind a cyclist as revealed by Griffith *et al.* (2014). (*b*) Reported drag area measurements from wind tunnel testing of cyclists in different positions and different studies: study 1 is Davies (1980), 2 is Kyle & Burke (1984), 3 is Martin *et al.* (1998), 4 is Padilla *et al.* (2000), 5 is Jeukendrup & Martin (2001), 6 and 7 are Garcia-Lopez *et al.* (2008), 8 is Gibertini & Grassi (2008), 9 is Underwood *et al.* (2011), 10 is Defraeye *et al.* (2010), 11 is Barry *et al.* (2014) and 12 is Barry *et al.* (2015).

(*a*)



(*b*)

S (km)	α (%)	t_{meas} (s)	V_{TTc} (m s^{-1})	t_{calc} (s)	Error (%)
0.00	0.0		14.0	0.000	
1.00	0.0		14.0	71.58	
2.00	0.20		13.8	144.2	
3.00	1.1		12.8	222.1	
4.00	1.8		12.1	304.5	
5.00	8.0		6.93	448.7	
6.00	11		5.41	633.5	
6.50	10.5	716.00	5.60	719.6	0.50
7.00	10		5.81	805.7	
8.00	1.6		12.3	886.7	
9.00	4.3		9.73	989.5	
10.0	4.7	1139.0	9.38	1096	3.7
11.0	5.1		9.04	1207	
12.0	8.3		6.75	1355	
13.0	0.20		13.8	1427	
13.5	8.0	1488.0	7.05	1501	0.80
14.0	8.2		6.81	1574	
15.0	2.5		11.4	1662	
16.0	0.0		14.0	1733	
17.0	0.0	1843.0	14.0	1805	2.0

Figure 5. (*a*) Road profile for the mountain type individual time trial of stage 18 in tour de France 2016 between Sallanches and Megève (Photo credits: AFP/Presse Sport). (*b*) Table of comparison for the race of the winner C. Froome: s is the distance from departure, α the slope of the road average over a km, t_{meas} is the time measured during the race at 4 different locations (6.5 km, 10 km, 13.5 km and arrival), V_{TTc} is the velocity computed using (3.7), t_{calc} is the time calculated at each km. The last column compares t_{calc} and t_{meas}.

this equation can be re-written as

$$\left[\frac{V_{TTc}(s)}{V_{TT}}\right]^3 + F\alpha(s)\left[\frac{V_{TTc}(s)}{V_{TT}}\right] = 1, \tag{3.6}$$

where $V_{TTc}(s)$ is the velocity at the location s and $F = MgV_{TT}(T)/P_{max}(T)$. Using Viete's substitution, $V_{TTc}(s)/V_{TT} = Y - \alpha F/3Y$ (3.6) is transformed into the quadratic form

https://doi.org/10.1017/jfm.2020.1022 Published online by Cambridge University Press

$Z^2 - Z - (\alpha F/3)^3 = 0$, where $Z = Y^3$. Finally, one gets the exact solution for the velocity as a function of the slope α

$$\frac{V_{TTc}(\alpha)}{V_{TT}} = \left(\frac{1+\sqrt{1+4(\alpha F/3)^3}}{2}\right)^{1/3} - \frac{\alpha F/3}{\left(\dfrac{1+\sqrt{1+4(\alpha F/3)^3}}{2}\right)^{1/3}}. \tag{3.7}$$

In the small slope limit ($\alpha F/3 \ll 1$), this expression reduces to $V_{TTc}(\alpha) = V_{TT}(1 - \alpha F/3)$. The velocity decrease is thus directly proportional to the slope. It also depends on the athlete characteristics via the parameter $F = MgV_{TT}/P_m = (2M^3g^3/\rho SC_D P_m^2)^{1/3}$. The larger this parameter the larger the relative velocity decrease. In the case of Froome in this stage, one finds $P_{max} = 409.3$W, $V_{TT} = 13.97$ m s^{-1} (50.3 km h^{-1}) and $F = 22.1$.

Using the slopes $\alpha(s)$ in the different sections of the stage presented in figure 5(*a*), one can then evaluate the corresponding velocity $V_{TTc}(\alpha(s))$ using (3.7) and deduce the time $t_{calc}(s) = \int_0^s \mathrm{d}s'/V_{TTc}(\alpha(s'))$. This time is presented in the fifth column of figure 5(*b*). It can be compared to the 4 intermediate times measured during the race at the locations 6.5 km, 10 km, 13.5 km and 17 km. These times are reported in the third column t_{meas}. The error between the estimated and the actual time never exceed 3 % and the mean velocity we calculate is 33.4 km h^{-1}, very close to the 33.2 km h^{-1} reported in table 1.

3.2. *High mountains*

The characteristics of some emblematic mountain climbs associated with Tour de France together with the records reproduced from the book of Vayer & Portoleau (2001) are presented in table 2.

The typical mean slope is 8 %, the length varies from 5 to 19 km and the mean velocity for the fastest climbers is 22 ± 2 km h^{-1}. At this velocity, the power consumed through aerodynamical friction is typically 20–30 W while the power developed by the rider is still of the order of 400 W. We thus first neglect the aerodynamical drag in our analysis of mountain climb. In the steady regime, (3.4) reduces to the balance between the maximal generated muscle power $P_m = P_{max}(T)$ and the climbing term $Mg\alpha V$. This balance leads to the expression of the climbing velocity V_{MT0}:

$$V_{MT0}(T) = \frac{P_{max}(T)}{Mg\alpha}. \tag{3.8}$$

Using (3.3) with $\tau = 32$ s, $\gamma = 0.0886$ and $\Pi = 9.7$ W kg^{-1} we estimate $P_{max}(T)$ for all the riders in table 2 (column 9) and deduce the velocity $V_{MT0}(T)$ (column 10) with (3.8) taking $M_b = 10$ kg. The predicted velocity is always larger than the actual velocity by typically 20 %–30 %.

To obtain a better prediction, one needs to account for the aerodynamic drag and for the rolling resistance. In the equation $P_m = 1/2\rho SC_D V^3 + Mg\alpha V + \mu MgV$, the dominant term in climbing is the one associated with α. Using a perturbative method, we get the correction associated with the extra two terms

$$V_{MT1}(T) = V_{MT0}(T)\left(1 - \frac{\mu}{\alpha} - \frac{1}{2}\frac{\rho SC_D V_{MT0}^2}{Mg\alpha}\right). \tag{3.9}$$

In the limit $\alpha \gg 1$ the corrective terms vanish and we recover $V_{MT1} = V_{MT0}$. With $\mu = 0.0032$, $\rho = 1.2$ kg m^{-3} and $SC_D = 0.25$ m^2, the corrected velocity $V_{MT1}(T)$ is calculated

https://doi.org/10.1017/jfm.2020.1022 Published online by Cambridge University Press

MT	Slope (%)	D (km)	Record holder	T (m s)	$\bar{V}_{MT}$ (km h^{-1})	L_c (m)	M_c (kg)	P_{max} (W)	V_{MT0} (km h^{-1})	V_{MT1} (km h^{-1})	Error (%)
The Pyrenees											
Tourmalet (ouest)	7.5	18.7	T. Pinot	54′ 57″	20.7	1.80	63	363	24.3	20.2	1.0
Luz Ardiden	7.4	13.8	R. Laiseka	37′ 20″	22.2	1.84	60	366	25.9	20.8	6.0
Plateau de Beille	7.8	15.9	M. Pantani	43′ 30″	21.9	1.72	57	340	23.8	19.8	9.6
Soulor (nord)	8.1	8.5	R. Virenque	25′ 15″	20.4	1.79	65	418	25.2	21.1	4.6
Hautacam	7.7	13.8	B. Riis	34′ 35″	23.95	1.84	71	437	25.7	21.4	10.4
Aspin (ouest)	7.6	5	L. Piepoli	14′ 00″	21.4	1.69	54	374	28.2	21.5	0.73
The Alps											
La planche des belles filles	9	5.8	G. Bennett	17′ 21″	20.1	1.80	58	391	23.4	20.1	0.44
Ventoux (sud)	8.6	15.9	M. Pantani	46′	20.7	1.72	57	337	21.5	18.6	10.0
Alpe d'Huez	8.1	13.8	M. Pantani	36′ 50″	22.5	1.72	57	348	23.5	19.8	12
Izoard (sud)	7.4	9.1	M. Indurain	26′ 30″	20.6	1.86	76	485	28.0	22.7	10.3
Izoard	7	13.8	W. Barguil	37′ 53″	21.9	1.82	61	371	27.4	21.2	2.6
Galibier (nord)	6.9	17.9	M. Pantani	48′ 20″	22.2	1.72	57	335	26.6	20.5	7.4
Madeleine	7.8	19	R. Virenque	56′	20.3	1.97	65	373	23.4	19.9	2.3

Table 2. Some classic mountain climbs and their records reproduced from Vayer & Portoleau (2001). The average slope is indicated in the second column, the length of the climb D in the third and the record time T in the fifth. From these values we calculate the average velocity $\bar{V}_{MT} = D/T$ (column 6). The record holder is given in 4 and his height and mass in 7 and 8. Using (3.3) we evaluate the power $P_{max}(T)$ in column 9. The velocity V_{MT0} predicted by (3.8) is given in column 10. The corrected velocity V_{MT1} accounting for the aerodynamic drag and rolling resistance is calculated with (3.9) in column 11. The error between the predicted velocity V_{MT1} and the actual velocity $\bar{V}_{MT}$ is indicated in the last column.

and the results are listed in column 11 of table 2. The error reported in the last column reveals that the corrected velocity is closer to reality (less than 10 %).

3.3. *The sprint*

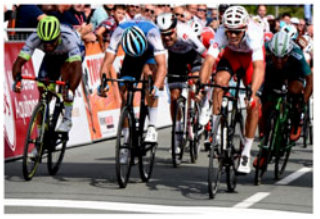
The last term of (3.4) is associated with the acceleration of the rider. This term has been neglected so far since we have only considered phases where the velocity remains mainly constant. This is no longer the case for sprints. Some characteristics of a road sprint are presented in figure 6: the power output recorded in a bunch sprint performed in a professional road cycling competition is presented in figure 6(*b*) together with the corresponding velocity (Menaspa 2015). Interestingly, the power data were recorded during a successful sprint. In this example the duration of the final sprint is 11 s, and the mean power is 1020 W (peak power 1248 W), with a maximal recorded speed of 66 km h^{-1}. The authors also report the intensity recorded before the sprint. The cyclist rode at an average power output of 490 W in the last 3 min. The data collected over a larger number of sprinters are gathered in the table presented in figure 6(*c*).

Since the slope of the road α is small for sprints, their dynamics is described by a simplified version of (3.4): $\mathrm{d}/\mathrm{d}t(1/2MV^2) + 1/2\rho S C_D V^3 = P_m$. This nonlinear equation can be turned into a linear equation in V^3 by replacing the time derivative term $\mathrm{d}/\mathrm{d}t(1/2MV^2)$ by its spatial equivalent $\mathrm{d}(1/3MV^3)/\mathrm{d}s$

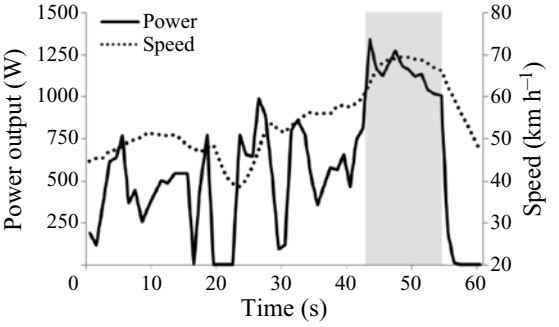
$$\frac{\mathrm{d}V^3}{\mathrm{d}s} + \frac{V^3}{L_{sprint}} = \frac{3P_m}{M}, \tag{3.10}$$

https://doi.org/10.1017/jfm.2020.1022 Published online by Cambridge University Press

(*a*)



(*b*)



(*c*)

	Whole sprint	Peak data
Power (W)	1020 ± 77 (865–1140)	1248 ± 122 (989–1443)
Power (W·kg^{-1})	14.2 ± 1.1 (12.2–15.8)	17.4 ± 1.7 (13.9–20.0)
Cadence (r.p.m.)	110 ± 5 (100–117)	114 ± 5 (102–121)
Speed (km·h^{-1}) #	63.9 ± 3.8 (53.7–69.1)	66.1 ± 3.4 (57.1–70.6)

Figure 6. (*a*) Example of final sprint in a road race. Photo credits: T. Vergouwen. (*b*) Example of power output and speed recorded at the end of a road race. The final sprint is highlighted in grey. Reproduced from Menaspa (2015). (*c*) Characteristics of road sprints in professional competitions; mean ± standard deviation (range). Reproduced from Menaspa *et al.* (2015).

where $L_{sprint} = 2M/3\rho SC_D$ appears as the characteristic length scale of sprints. According to the data presented in figure 6, before launching the sprint the power is of the order of $P_{m0} \approx 490$ W, which leads in the steady limit to the velocity before sprint $V_0 \approx (2P_{m0}/\rho SC_D)^{1/3}$. With $SC_D \approx 0.25$ m^2 this leads to $V_0 = 53$ km h^{-1}. When the sprint is launched the power increases to $P_{sprint} \approx 1100$ W and the maximum velocity which could be reached in steady state is $V_{sprint} = (2P_{sprint}/\rho SC_D)^{1/3}$. The value of the aerodynamic coefficient in the sprint regular position is 0.3 m^2 (Blocken *et al.* 2019). We thus deduce $V_{sprint} \approx 66$ km h^{-1}. The exact solution of (3.10) is

$$V(s) = V_{sprint}\left[1 - \mathrm{e}^{-s/L_{sprint}} + \left(\frac{V_0}{V_{sprint}}\right)^3 \mathrm{e}^{-s/L_{sprint}}\right]^{1/3}. \tag{3.11}$$

This exact solution reveals that the acceleration from V_0 to V_{sprint} requires the characteristic length L_{sprint}. With $M = 80$ kg and $SC_D \approx 0.3$ m^2 one deduces that the sprints must start at least 150 m before the finish line. At an average speed of 60 km h^{-1}, this distance is covered over 9 s, which is the characteristic duration of sprints (Menaspa *et al.* 2013). The characteristic velocities V_0 and V_{sprint} as well as the duration of actual sprints are thus correctly described by (3.10).

3.4. *The descent*

In a first approximation, we consider that, during descents, cyclists mainly rest ($P_m \approx 0$) and change their position in order to maximize their velocity. Different positions have been tested as illustrated in figure 7 reproduced from the detailed study of Blocken *et al.* (2018*a*). Since the muscle power is null and the regime steady, the characteristic velocity in the descent V_{D0} results from the balance between the propulsive gravitational power $Mg(-\alpha)V_{D0}$ and the resistive aerodynamical friction

$$V_{D0} = \sqrt{\frac{2Mg(-\alpha)}{\rho SC_D}}. \tag{3.12}$$

In their study, Blocken *et al.* (2018*a*) considered the descent of C. Froome in stage 8 of Tour de France 2016. This stage ended with the descent of Peyresourde, which is steep

https://doi.org/10.1017/jfm.2020.1022 Published online by Cambridge University Press

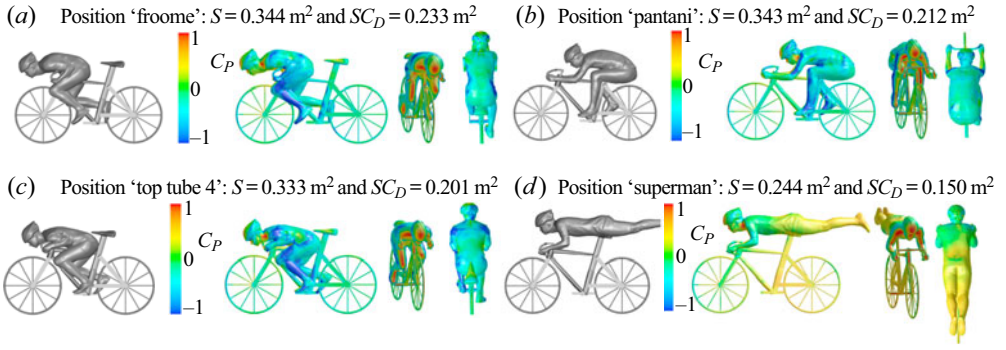


Figure 7. Four different positions used during descents with the corresponding static pressure coefficient $C_P = 2(P - P_0)/\rho V_0^2$ on cyclist and bicycle surfaces. Here, P is the static pressure, P_0 the atmospheric pressure and V_0 the velocity of the centre of mass. The frontal area S and the drag area SC_D are also indicated for four significantly different positions: (*a*) the Froome position, (*b*) the Pantani position, (*c*) top tube 4 and (*d*) the superman position. This figure is reproduced from Blocken *et al.* (2018*a*).

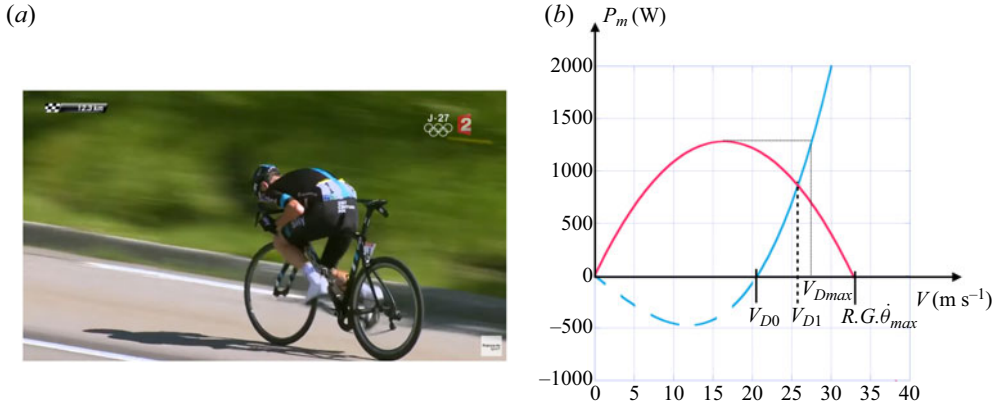


Figure 8. (*a*) C. Froome in stage 8 of Tour de France 2016 pedalling during the descent of Peyresourde. Photo credits: France TV. (*b*) Impact of the pedalling on the speed during descent. The needed power (3.13) is presented in blue and the muscle power (3.14) is presented with a pink solid line.

with a regular slope ($\alpha = -8\,\%$) and is not characterized by sharp bends. On the day of the descent, the weather conditions were good and the road surface was dry. Near the very end of this stage, just before the top of Peyresourde, C. Froome accelerated and broke away from the group. During part of the descent, he adopted the position shown in figure 7(*a*) and achieved speeds up to 90 km h^{-1}. Since $M_c = 66$ kg for Froome, we use $M = 76$ kg, $\alpha = -8\,\%$ and $SC_D = 0.233$ in (3.12) to evaluate $V_{D0} = 20.6$ m s^{-1} $= 74$ km h^{-1} which is smaller than the reported value. The difference is due to the injected power: the 'Froome' position is used instead of the 'superman' position since it allows for pedalling and C. Froome was indeed pedalling during the descent of Peyresourde (figure 8*a*).

To quantify the effect of pedalling during descent, one can rewrite (3.4) in the steady state limit of a descent in the form

$$P_m = \tfrac{1}{2}\rho S C_D V (V^2 - V_{D0}^2). \tag{3.13}$$

https://doi.org/10.1017/jfm.2020.1022 Published online by Cambridge University Press

When $P_m = 0$ we recover $V = V_{D0}$ and when P_m is positive, the velocity increases. This first relationship between the injected power and the velocity is plotted with a blue line in figure 8(*b*), using $SC_D = 0.233$, $\rho = 1.2$ kg m^{-3} and $V_{D0} = 20.6$ m s^{-1}. As already discussed, the injected power also depends on the pedalling rate $\dot{\theta}$ (which is related to the velocity by the relation $V = RG\dot{\theta}$, where R is the radius of the wheel and G is the gear ratio). Typically in mountain stages, professional cyclists have a maximal gear ratio $G = 54/11 = 4.91$. This second relationship between the injected power and the velocity takes the form

$$P_m = 8\Pi M_c \frac{V}{RG\dot{\theta}_{max}}\left(1 - \frac{V}{RG\dot{\theta}_{max}}\right). \tag{3.14}$$

In this expression we have used the relationship $P_{max} = 2\Pi M_c$ that applies for short efforts after rest (limit of (3.3) when $T = 0$). This equation is presented with a pink solid line in figure 8(*b*), using $\Pi = 9.7$ W kg^{-1}, $M_c = 66$ kg, $G = 4.91$, $R = 0.334$ m and $\dot{\theta}_{max} = 18.8$ rad s (which corresponds to $\dot{\theta}_{max} = 180$ r.p.m.). The first observation is that power can only be used if the maximal pedalling velocity $RG\dot{\theta}_{max}$ is larger than V_{D0}. This condition imposes a minimal gear ratio $G_{min} = V_{D0}/R\dot{\theta}_{max}$. In the case of Froome, we get $G_{min} = 3.3$. The typical gear ratio used in mountain stages $G = 54/11 = 4.91 > G_{min}$ ensures that power can be injected during the descent. Once this condition is fulfilled, the effect of the injected power on the velocity is obtained by equating the needed power (3.13) and the injected power (3.14). This balance corresponds to the crossing point of the blue and pink lines in figure 8(*b*). One reads $V_{D1} = 25.5$ m s^{-1} which is 91.8 km h^{-1}. A value much closer to the one observed in 2016 during the descent of Froome. One also observes in figure 8(*b*) that there exists a maximal velocity of descent V_{Dmax} obtained when the injected power is maximal. In the case of Froome in Peyresourde we read $V_{Dmax} = 27.4$ m s^{-1} = 98.8 km h^{-1}. In order to achieve this maximal velocity of descent he should use a gear ratio such that $RG_{max}\dot{\theta}_{max} = 2V_{Dmax}$ that is $G_{max} = 8.7$. A huge modification (extra kg during the climb) for a modest gain. One major characteristic of descent is breaking, which is not addressed here but constitutes a perspective of this work.

4. Phase diagram for road cycling

Up to now, the best descender does not have a special jersey. In this section, we thus analyse the other phases identified in § 3 and propose a phase diagram for road cycling.

4.1. *What is a climber?*

In the peloton, climbers are identified and usually associated with light weight together with a large power to mass ratio (Lucia *et al.* 2000; Lucia, Hoyos & Chicharro 2001) such as Marco Pantani (1.72 m, 57 kg), Alberto Contador (1.76 m, 61 kg), Nairo Quintana (1.67 m, 58 kg), Egan Bernal (1.75 m, 60 kg).

On the physical side, one way to define a climber is to discuss the validity domain of (3.8) for V_{MT0}: in the steady regime, (3.8) only holds if the power dissipated by aerodynamical forces can be neglected. Since $V_{MT0} \propto 1/\alpha$ the smaller the slope the larger the velocity. This implies that (3.8) only holds above a critical slope $\alpha^\star$ for which the gravitational power request $Mg\alpha^\star V(\alpha^\star)$ exactly balances the power dissipated by the aerodynamical friction $1/2\rho SC_D V(\alpha^\star)^3$ (we neglect solid friction to simplify

https://doi.org/10.1017/jfm.2020.1022 Published online by Cambridge University Press

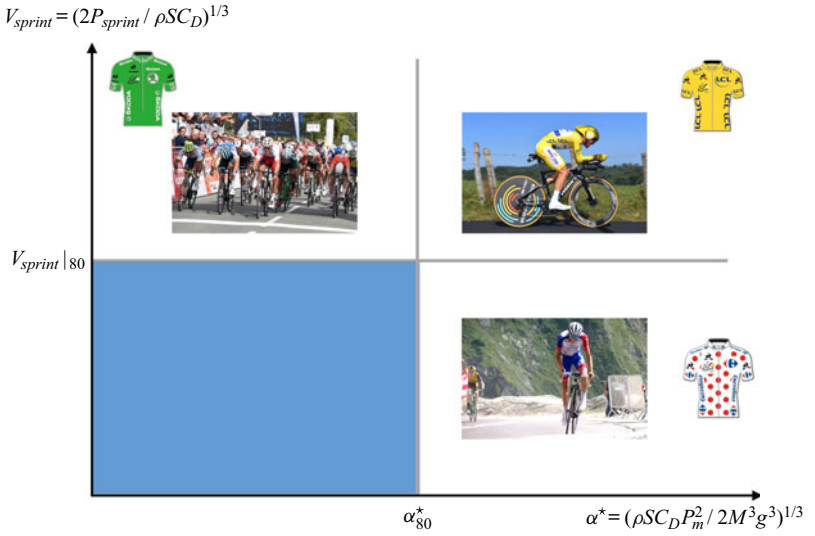


Figure 9. Phase diagram for road cycling. Photo credits: T. Vergouwen/AFP/Presse Sport.

the discussion). This balance leads to the following expression:

$$\alpha^\star = \left(\frac{P_m}{M}\right)^{2/3} \left(\frac{\rho SC_D}{2Mg^3}\right)^{1/3}. \tag{4.1}$$

This angle separates the flat region ($\alpha < \alpha^\star$) where the aerodynamics dominates gravity from the mountain region ($\alpha > \alpha^\star$) where gravity dominates. The limit $\alpha^\star = \infty$ corresponds to $g = 0$ where the mountains do not influence the velocity anymore. The angle $\alpha^\star$ also depends on the athlete characteristics (P_m, M, SC_D) and one deduces from the zero g discussion that climbers have a large $\alpha^\star$.

Equation (4.1) shows that, in order to achieve a large $\alpha^\star$, one needs a large power to mass ratio (first term) but also a small mass (second term), thus recovering what has been reported for climbers by Lucia *et al.* (2000).

Since the power to mass ratio can be approached by the heuristic equation (3.3), one deduces that, for a climb, which lasts in general $T \approx 30$ min $\gg \tau$, the power to mass ratio reduces to $P_m/M_c = \Pi[1 - \ln(T/\tau)^\gamma] \approx 0.64\Pi M_c/M$, using $\gamma = 0.0886$ and $\tau = 32$ s.

If N stands for the number of cyclists of the Tour de France, one can define the climbers as the best 20 % of the peloton by a critical angle $\alpha^\star_{80}$ such that 80 % of the peloton has a lower angle $\alpha^\star$. One can then use a scale of $\alpha^\star$ as the horizontal axis of the diagram presented in figure 9. The riders with a personal $\alpha^\star$ larger than $\alpha^\star_{80}$ are climbers.

4.2. *What is a sprinter?*

The first remark about sprinters is that they win lots of stages: the examination of the sprint results in several grand tours (2008–2011) indicates that 79 stages (31 % of 252 total number of stages) were won by only 24 sprinters. Five sprinters won 54 stages of which 1 sprinter won 30 stages (Menaspa *et al.* 2013). Mark Cavendish (70 kg), Peter Sagan (73 kg), Erik Zabel (69 kg) are some emblematic figures of this discipline.

On the physical side, according to (3.10), the best sprinter is the one with the largest peak velocity $V_{sprint} = (2P_{sprint}/\rho SC_D)^{1/3}$. A sprinter is thus characterized by a large absolute

https://doi.org/10.1017/jfm.2020.1022 Published online by Cambridge University Press

power and does not depend on the power to mass ratio. What we know from figure 3(*c*) is that the maximal power is obtained over a short period corresponding to an anaerobic effort. Since sprints occur at the end of a race that last a few hours, a sprinter must be protected by his team in order to keep his energy for the last hundreds of metres. What we also learn from 3(*c*) is that the maximal value of the power depends on the cyclist. Always using (3.3), we can evaluate the power P_{sprint} with $T = 10$ s and we find $P_{sprint} = 1.70\Pi M_c$. As we did for climbers, the associated velocity V_{sprint} can be calculated for all the riders in the peloton in order to evaluate $V_{sprint}|_{80}$ such that 80 % of the peloton has a lower peak velocity. The sprinters can then be defined as the ones who verify: $V_{sprint} > V_{sprint}|_{80}$. The vertical axis of the diagram presented in figure 9 presents this classification.

4.3. *The 3 jerseys*

The phase diagram presented in figure 9 is thus composed of two axes, the horizontal one dedicated to climbers and the vertical axis to sprinters. This diagram defines four different regions and we need to discuss the associated physical properties to understand the origin of the three jerseys: to be on the right hand-side of the diagram, a cyclist must have $\alpha^\star > \alpha^\star_{80}$, which implies having a large $P_m^2/M^3 = (P_m/M)^2/M$. In other words, a climber is defined by both a large power to mass ratio P_m/M and a small mass.

On the other hand, to be on the upper part of the diagram, a cyclist must have a large power P_{sprint} and a small drag area SC_D. Since the power scales with the mass, a large mass is expected to be in the upper part.

The upper-right part is populated with a category of cyclists who have both a large power to mass ratio and who are able to develop a large power. This rather rare combination defines TT specialists and very complete cyclists, which are the qualities recognized for Tour winners.

The phase diagram for road cycling thus has three optimal regions, occupied by three different physics and physiological characteristics and which are associated with three different jerseys: the green for the best sprinter (top left), the polka dot for the best climber (bottom right) and the yellow for the more complete one (top right).

Usually, the three jerseys are for three different cyclists but, depending on the route of the grand tour, one can have some overlap between these different regions. In 2019, the results presented in figure 1 reveal that the three jerseys winners were indeed different in Tour de France and in Giro but, for the Vuelta, the leader Primoz Roglic was also the best sprinter.

Since 1903, over the 106 Tour de France we observe only one exception, in 1969, where Eddy Merckx won the three jerseys (we thank P. Odier for this historical remark).

4.4. *Phase diagram for the Tour de France 2017*

To construct the phase diagram of Tour de France 2017, one needs to determine $\alpha^\star$ and V_{sprint} for each cyclist involved in the race. According to the discussions presented in §§ 4.1 and 4.2, one needs to determine the individual value of Π. We use the first stage of the Tour 2017, which was a flat time trial with $D = 14$ km. From the average velocity $\bar{V}_{TT}$ measured during the race for each rider, we calculate the individual value $2\Pi = \rho SC_D \bar{V}_{TT}^3/[M_c(1 - \gamma \ln(D/\tau \bar{V}_{TT}))]$. This expression is obtained using (3.5) and (3.3). This value is then used to evaluate the two characteristics

$$\alpha^\star = \left(0.64\Pi \frac{M_c}{M}\right)^{2/3} \left(\frac{\rho SC_D}{2Mg^3}\right)^{1/3} \quad \text{and} \quad V_{sprint} = \left(\frac{3.4\Pi M_c}{\rho SC_D}\right)^{1/3}. \tag{4.2a,b}$$

https://doi.org/10.1017/jfm.2020.1022 Published online by Cambridge University Press

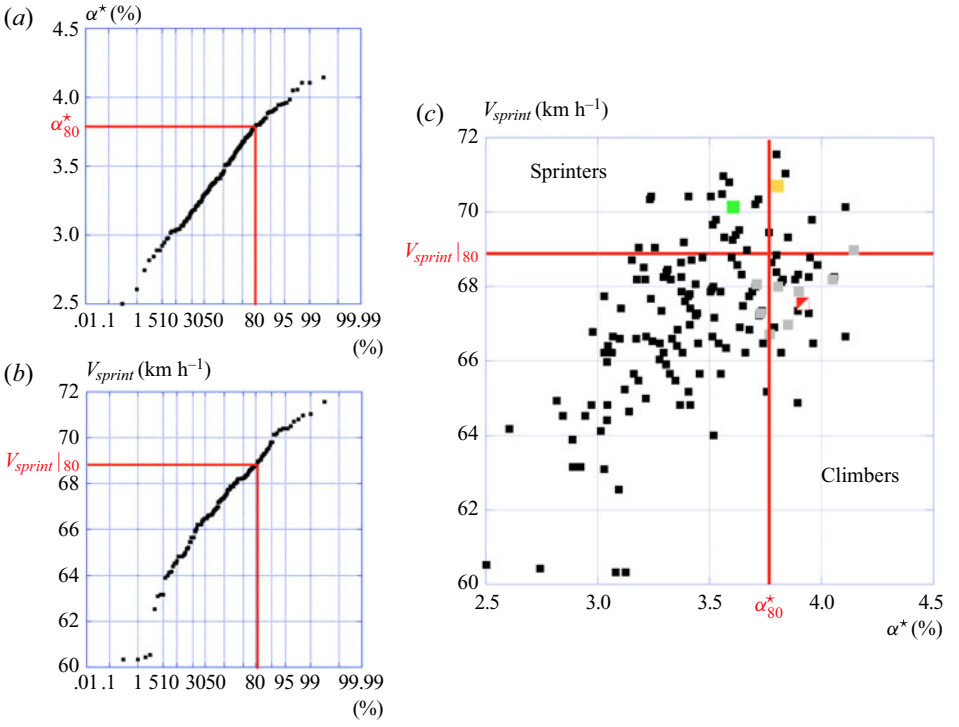


Figure 10. Phase diagram for the Tour de France 2017: (*a*) determination of $\alpha^\star_{80}$, (*b*) determination of $V_{max}|_{80}$, (*c*) construction of the phase diagram for the Tour 2017: each black square corresponds to a cyclist. The winner C. Froome is indicated with a large yellow square, the green jersey M. Matthews is indicated with a large green square and the polka dot jersey W. Barguil with a large white and red square. The large squares in grey are used for the final top 10.

The mass M_c and the size L_c of each cyclist are listed in the Appendix. As we did throughout the article SC_D is taken constant to 0.25 m^2, $\rho = 1.2$ kg m^{-3} and $M_b = 10$ kg. From these values, one is able to evaluate $\alpha^\star$ and V_{sprint} for the whole peloton.

The cumulative distribution of $\alpha^\star$ is presented in figure 10(*a*). One observes that $\alpha^\star$ varies from 2.5 % to 4.2 % and we extract the value $\alpha^\star_{80} = 3.77$ %. Only 20 % of the riders have a higher $\alpha^\star$. The cumulative distribution of V_{sprint} is presented in figure 10(*b*). The maximum velocity ranges from 60 to 72 km/h with $V_{max}|_{80} = 68.7$ km h^{-1}. So that only 20 % of the riders have a higher V_{max}.

Using these values, one can thus construct the phase diagram of the Tour 2017 which is presented in figure 10(*c*): the three jerseys of C. Froome (yellow square), M. Matthews (green square) and R. Bargil (white and red square) stand in the three different regions discussed in § 4.3. We also report, with grey squares, the locations of the riders who finished in the top 10 of the general classification (2-R.Urán, 3-R. Bardet, 4-M. Landa, 5-F. Aru, 6-D. Martin, 7-S. Yates, 8-L. Meintjes, 9-A. Contador, 10-W. Barguil). Clearly they are in the 'climber' zone, which underlines the fact that the Tour 2017 had a hilly design: 11 of the 21 stages were either medium mountain SMT (6) or high mountain MT (5).

https://doi.org/10.1017/jfm.2020.1022 Published online by Cambridge University Press

5. Conclusion and perspectives

In this paper, we first establish the equation of motion of a road cyclist and show that it is able to account for the data measured during Tour de France for the four different 'disciplines': time trial, climbing, sprint and descent. Using this equation, we then discuss the physics of the phases with continuous propulsion (time trial, climbing, sprint) and propose a phase diagram for road cycling which allows for the definition of three optimal areas, connected to the three different jerseys. This analysis is applied to the Tour de France 2017 and is shown to be consistent with actual data.

This work on the physics of cycling can be completed in different directions:

(i) We have only discussed individual phases. Collective effects, such as the ones at play in peloton, induce a very stimulating physics which has just started to be considered (Blocken *et al.* 2018*b*; Belden *et al.* 2019).
(ii) Team strategy is known to have a major effect in the final ranking of a grand tour.

This team strategy, which leads to an optimization of the performance of the leader, is an open field as far as physics is concerned.

(i) We have only considered phases were the cyclist uses his maximal available power. The issue of energy management during a race is completely open.
(ii) The state of the road does not play a major role in our analysis. However, it is known to be important for some special races, such as the Paris–Roubaix, which is famous for rough terrain and cobblestones, or pavé (setts). The terrain has led to the development of specialized frames, wheels and tyres. If one had to adapt the model to analyse Paris–Roubaix, the friction term P_f should be differently discussed.
(iii) For the descent, we have not discussed the question of breaking associated with turns. If one had to study the evolution of speed in descent, breaking should obviously be considered.
(iv) All the study is conducted assuming that the bikes have gears which allow the rider to keep his optimal physiological pedalling rate. Since there are no gears in track cycling, the model developed only applies to road cycling. A similar study must be conducted for track cycling.

Finally, all sport uncertainties such as motivation, resistance to pressure, wind and weather in general have been neglected in our discussion. We just propose the view of physicists and do not pretend to replace the living side of sport.

Acknowledgements. We first deeply thank S. Dorel, D. Burton, T. Crouch and B. Blocken for allowing us to use some of their work. We also thank P. Odier for his careful reading of the initial manuscript and for all his corrections and meaningful suggestions. They all contributed to improve the overall quality of our work.

Declaration of interests. The authors report no conflict of interest.

Author ORCIDs.
Christophe Clanet https://orcid.org/0000-0003-2448-0443.

Appendix. Riders of the Tour de France 2017

The table below presents the list of the riders of the Tour de France 2017 in alphabetic order. For each of them we indicate their team, their age, height L_c and mass M_c (reproduced from the website https://www.google.fr/amp/s/todaycycling.com/tour-de-france-2017-presentation-coureurs-age-poids-taille/amp/). Their average velocity $\bar{V}_{TT}$ during the first stage of the Tour 2017, which was a flat time trial run over a distance

https://doi.org/10.1017/jfm.2020.1022 Published online by Cambridge University Press

Name	Team	Age (y.o.)	Lc (m)	Mc (kg)	$\bar{V}_{TT}$ (m s^{-1})
ALBASINI Michael	ORICA-Scott	36	1.72	65	13.910
AMADOR Andrey	Movistar	30	1.81	73	14.120
ARNDT Nikias	Team Sunweb	25	1.88	77.5	14.279
BACKAERT Frederik	Wanty-Groupe Gobert	27	1.88	77	13.44
BAKELANTS Jan	AG2R La Mondiale	31	1.77	67	13.60
BARDET Romain	AG2R La Mondiale	26	1.84	65	13.79
BARGUIL Warren	Team Sunweb	25	1.83	60	13.68
BAUER Jack	Quick-Step Floors	32	1.91	74	13.81
BENNATI Daniele	Movistar	36	1.83	71	13.72
BENNETT George	LottoNL-Jumbo	27	1.80	58	13.19
BENOOT Tiesj	Lotto Soudal	23	1.90	72	13.47
BETANCUR Carlos	Movistar	27	1.67	65	13.75
BETTIOL Alberto	Cannondale-Drapac	23	1.80	69	13.77
BEVIN Patrick	Cannondale-Drapac	26	1.80	75	13.05
BOASSON HAGEN Edvald	Dimension Data	30	1.85	75	14.28
BODNAR Maciej	BORA – hansgrohe	32	1.86	70	14.04
BOLE Grega	Bahrain Merida	31	1.77	68	13.40
BOUHANNI Nacer	Cofidis	26	1.75	66	12.64
BRAMBILLA Gianluca	Quick-Step Floors	29	1.70	57	13.46
BUCHMANN Emanuel	BORA – hansgrohe	24	1.81	62	13.94
BURGHARDT Marcus	BORA – hansgrohe	33	1.89	75	13.11
CALMEJANE Lilian	Direct Energie	24	1.84	69	13.76
CARUSO Damiano	BMC Racing Team	29	1.79	67	13.84
CASTROVIEJO Jonathan	Movistar	30	1.71	62	14.22
CAVENDISH Mark	Dimension Data	32	1.75	70	13.08
CHAVANEL Sylvain	Direct Energie	37	1.81	73	13.83
CHAVES Johan Esteban	ORICA-Scott	27	1.64	55	13.49
CIMOLAI Davide	FDJ	27	1.85	69	13.15
CINK Ondrej	Bahrain Merida	26	1.80	66	13.49
CLAEYS Dimitri	Cofidis	30	1.89	77	13.40
CLARKE Simon	Cannondale-Drapac	30	1.75	63	13.64
COLBRELLI Sonny	Bahrain Merida	27	1.76	71	14.05
CONTADOR Alberto	Trek – Segafredo	34	1.76	61	13.75
CURVERS Roy	Team Sunweb	37	1.88	73	12.77
DE GENDT Thomas	Lotto Soudal	30	1.77	69	13.44
DE KORT Koen	Trek – Segafredo	34	1.79	69	13.75
DE MARCHI Alessandro	BMC Racing Team	31	1.80	65	13.95
DEGAND Thomas	Wanty-Groupe Gobert	31	1.76	63	13.29
DEGENKOLB John	Trek – Segafredo	28	1.80	77	13.81
DELAGE Mickaël	FDJ	31	1.80	70	13.37
DEMARE Arnaud	FDJ	25	1.82	78	13.81
DOMONT Axel	AG2R La Mondiale	26	1.79	65	13.46
DURBRIDGE Luke	ORICA-Scott	26	1.87	78	12.22
EDET Nicolas	Cofidis	29	1.76	60	13.67
ERVITI Imanol	Movistar	33	1.89	75	13.83
FELLINE Fabio	Trek – Segafredo	27	1.75	68	13.98
FRANK Matthias	AG2R La Mondiale	30	1.76	64	13.55
FROOME Christopher	Team Sky	32	1.86	69	14.34
FUGLSANG Jakob	Astana Pro Team	32	1.82	68	13.75
GALLOPIN Tony	Lotto Soudal	29	1.80	70	12.20

https://doi.org/10.1017/jfm.2020.1022 Published online by Cambridge University Press

Name	Team	Age (y.o.)	Lc (m)	Mc (kg)	$\bar{V}_{TT}$ (m s^{-1})
GASTAUER Ben	AG2R La Mondiale	29	1.90	73	13.49
GAUTIER Cyril	AG2R La Mondiale	29	1.68	64	13.11
GESCHKE Simon	Team Sunweb	31	1.70	64	13.85
GESINK Robert	LottoNL-Jumbo	31	1.89	70	14.06
GILBERT Philippe	Quick-Step Floors	34	1.79	67	14.08
GOGL Michael	Trek – Segafredo	23	1.86	70	13.53
GREIPEL André	Lotto Soudal	34	1.84	75	13.71
GRIVKO Andre	Astana Pro Team	33	1.81	70	14.26
GRMAY Tsgabu	Bahrain Merida	25	1.75	63	13.53
GROENEWEGEN Dylan	LottoNL-Jumbo	24	1.77	70	12.97
GRUZDEV Dmitriy	Astana Pro Team	31	1.83	72	13.75
GUARNIERI Jacopo	FDJ	29	1.89	78	13.05
HALLER Marco	Katusha – Alpecin	26	1.78	72	13.29
HANSEN Adam	Lotto Soudal	36	1.86	75	12.92
HAYMAN Mathew	ORICA-Scott	39	1.90	78	13.65
HENAO Sergio Luis	Team Sky	29	1.69	61	13.46
HERRADA Jesús	Movistar	26	1.83	72	13.94
HOLLENSTEIN Reto	Katusha – Alpecin	31	1.97	80	13.99
HOWSON Damien	ORICA-Scott	24	1.88	68	13.90
IMPEY Daryl	ORICA-Scott	32	1.81	70	14.24
IRIZAR Markel	Trek – Segafredo	37	1.82	73	13.64
IZAGIRRE Ion	Bahrain Merida	28	1.73	60	12.18
KEUKELEIRE Jens	ORICA-Scott	28	1.85	69	13.61
KITTEL Marcel	Quick-Step Floors	29	1.88	82	14.28
KIRYIENKA Vasil	Team Sky	35	1.82	69	14.41
KNEES Christian	Team Sky	36	1.94	81	13.72
KONOVALOVAS Ignatas	FDJ	31	1.90	75	13.85
KREUZIGER Roman	ORICA-Scott	31	1.83	65	13.72
KRISTOFF Alexander	Katusha – Alpecin	29	1.81	78	13.99
LAENGEN Vegard Stake	UAE Team Emirates	28	1.95	80	13.52
LAMMERTINK Maurits	Katusha – Alpecin	26	1.70	59	13.63
LANDA Mikel	Team Sky	27	1.73	60	13.56
LAPORTE Christophe	Cofidis	24	1.89	76	13.48
LATOUR Pierre	AG2R La Mondiale	23	1.80	64	14.15
LE GAC Olivier	FDJ	23	1.80	70	13.40
LEEZER Tom	LottoNL-Jumbo	31	1.85	76	13.40
LEMOINE Cyril	Cofidis	34	1.81	70	13.65
LUTSENKO Alexey	Astana Pro Team	24	1.75	70	14.09
MACHADO Tiago	Katusha – Alpecin	31	1.78	63	13.61
MAJKA Rafa	BORA – hansgrohe	27	1.73	62	13.81
MARTENS Paul	LottoNL-Jumbo	33	1.78	69	13.94
MARTIN Daniel	Quick-Step Floors	30	1.75	59	13.81
MARTIN Guillaume	Wanty-Groupe Gobert	24	1.73	55	13.13
MARTIN Tony	Katusha – Alpecin	32	1.85	75	14.39
MATÉ Luis Ángel	Cofidis	33	1.77	69	12.76
MATTHEWS Michael	Team Sunweb	26	1.80	72	14.22
MCCARTHY Jay	BORA – hansgrohe	24	1.74	63	13.53
MEINTJES Louis	UAE Team Emirates	25	1.73	61	13.51
MINNAARD Marco	Wanty-Groupe Gobert	28	1.78	65	13.11
MOINARD Amaël	BMC Racing Team	35	1.80	69	13.34

https://doi.org/10.1017/jfm.2020.1022 Published online by Cambridge University Press

Name	Team	Age (y.o.)	Lc (m)	Mc (kg)	$\bar{V}_{TT}$ (m s^{-1})
MOLLEMA Bauke	Trek – Segafredo	30	1.81	64	13.43
MORENO Daniel	Movistar	35	1.73	59	13.40
NAESEN Oliver	AG2R La Mondiale	26	1.84	71	13.46
NAVARRO Daniel	Cofidis	33	1.75	60	12.95
NIEVE Mikel	Team Sky	33	1.73	62	13.40
OFFREDO Yoann	Wanty-Groupe Gobert	30	1.89	68	13.29
PANTANO Jarlinson	Trek – Segafredo	28	1.73	61	13.83
PHINNEY Taylor	Cannondale-Drapac	26	1.97	82	14.26
PINOT Thibaut	FDJ	27	1.80	63	13.80
POLITT Nils	Katusha – Alpecin	23	1.92	80	13.92
POLJANSKI Pawel	BORA – hansgrohe	27	1.80	67	13.25
PORTE Richie	BMC Racing Team	32	1.72	62	13.84
QUINTANA Nairo	Movistar	27	1.67	59	13.83
ROCHE Nicolas	BMC Racing Team	32	1.78	70	13.48
ROGLIC Primoz	LottoNL-Jumbo	27	1.77	65	13.77
ROLLAND Pierre	Cannondale-Drapac	30	1.84	67	13.46
ROOSEN Timo	LottoNL-Jumbo	24	1.94	75	14.02
ROWE Luke	Team Sky	27	1.85	72	13.03
SABATINI Fabio	Quick-Step Floors	32	1.87	74	13.48
SAGAN Juraj	BORA – hansgrohe	28	1.73	65	13.19
SAGAN Peter	BORA – hansgrohe	27	1.84	73	14.15
SELIG Rüdiger	BORA – hansgrohe	28	1.88	80	13.14
SÉNÉCHAL Florian	Cofidis	23	1.79	76	13.35
SEPÚLVEDA Eduardo	Fortuneo-VVital Concept	26	1.73	61	13.55
SIMON Julien	Cofidis	31	1.76	65	13.29
SINKELDAM Ramon	Team Sunweb	28	1.93	77	13.49
SWIFT Ben	UAE Team Emirates	29	1.79	69	13.56
TALANSKY Andrew	Cannondale-Drapac	28	1.75	63	13.81
TEN DAM Laurens	Team Sunweb	36	1.84	69	13.63
TEUNISSEN Mike	Team Sunweb	24	1.84	73	13.92
THOMAS Geraint	Team Sky	31	1.83	71	14.52
TIMMER Albert	Team Sunweb	32	1.86	71	13.79
TRENTIN Matteo	Quick-Step Floors	27	1.79	74	14.36
ULISSI Diego	UAE Team Emirates	27	1.75	61	13.90
URAN Rigoberto	Cannondale-Drapac	30	1.73	63	13.63
VAN AVERMAET Greg	BMC Racing Team	32	1.81	74	13.91
VAN BAARLE Dylan	Cannondale-Drapac	25	1.87	78	13.88
VAN EMDEN Jos	LottoNL-Jumbo	32	1.86	74	14.29
VAN KEIRSBULCK Guillaume	Wanty-Groupe Gobert	26	1.92	85	12.98
VALGREN Michael	Astana Pro Team	25	1.79	71	13.73
VALVERDE Alejandro	Movistar	37	1.78	61	12.18
VANSPEYBROUCK Pieter	Wanty-Groupe Gobert	30	1.86	72	13.20
VERMOTE Julien	Quick-Step Floors	27	1.79	71	13.69
VOECKLER Thomas	Direct Energie	38	1.74	71	13.25
VUILLERMOZ Alexis	AG2R La Mondiale	29	1.74	60	13.64
WAGNER Robert	LottoNL-Jumbo	34	1.86	75	13.87
WELLENS Tim	Lotto Soudal	26	1.83	65	14.05
WYSS Danilo	BMC Racing Team	31	1.76	65	13.67
YATES Simon	ORICA-Scott	24	1.72	59	13.98
ZABEL Rick	Katusha – Alpecin	23	1.84	72	12.77
ZEITS Andrey	Astana Pro Team	30	1.89	73	13.11

https://doi.org/10.1017/jfm.2020.1022 Published online by Cambridge University Press

of 14 km in the streets of the city of Düsseldorf, is then given. This velocity is then used in § 4.4 to construct the phase diagram presented in figure 10.

References

Barry, N., Burton, D., Sheridan, J., Thompson, M.C. & Brown, N.A.T. 2014 Aerodynamic performance and riding posture in road cycling and triathlon. *Proc. Inst. Mech. Engrs* P **229** (1), 28–38.

Barry, N., Burton, D., Sheridan, J., Thompson, M.C. & Brown, N.A.T. 2015 Aerodynamic drag interactions between cyclists in a team pursuit. *Sports Engng* **18** (2), 93–103.

Belden, J., Mansoor, M.M., Hellum, A., Rahman, S.R., Meyer, A., Pease, C., Pacheco, J., Koziol, S. & Truscott, T.T. 2019 How vision governs the collective behaviour of dense cycling pelotons. *J. R. Soc. Interface* **16**, 20190197.

Blocken, B., van Druenen, T., Toparlar, Y. & Andrianne, T. 2018*a* Aerodynamic analysis of different cyclist hill descent positions. *J. Wind Engng Ind. Aerodyn.* **181**, 27–45.

Blocken, B., van Druenen, T., Toparlar, Y. & Andrianne, T. 2019 CFD analysis of an exceptional cyclist sprint position. *Sports Engng* **22** (1), 10.

Blocken, B., van Druenen, T., Toparlar, Y., Malizia, F., Mannion, P., Andrianne, T., Marchal, T., Maas, G.J. & Diepens, J. 2018*b* Aerodynamic drag in cycling pelotons: new insights by cfd simulation and wind tunnel testing. *J. Wind Engng Ind. Aerodyn.* **179**, 319–337.

Carrey, P. 2015 *Maillot à pois : 40 ans de bataille pour les sommets*. Direct velo.

Carrey, P., Turgis, D. & Endrizzi, L. 2019 *Giro*. Hugo Sport.

Chany, P. 1983 *La fabuleuse histoire du Tour de France*. O.D.I.L.

Crouch, T.N., Burton, D., Brown, N.A.T., Thompson, M.C. & Sheridan, J. 2014 Flow topology in the wake of a cyclist and its effect on aerodynamic drag. *J. Fluid Mech.* **748**, 5–35.

Crouch, T.N., Burton, D., LaBry, Z.A. & Blair, K.B. 2017 Riding against the wind: a review of competition cycling aerodynamics. *Sports Engng* **20**, 81–110.

Davies, C.T.M.. 1980 Effect of air resistance on the metabolic cost and performance of cycling. *Eur. J. Appl. Physiol.* **45**, 245–254.

Defraeye, T., Blocken, B., Koninckx, E., Hespel, P. & Carmeliet, J. 2010 Aerodynamic study of different cyclist positions: CFD analysis and full-scale wind-tunnel tests. *J. Biomech* **43** (7), 1262–1268.

Dorel, S., Hautier, C.A., Rambaud, O., Rouffet, D., Van Praagh, E., Lacour, J.-R. & Bourdin, M. 2005 Torque and power-velocity relationships in cycling: relevance to track sprint performance in world-class cyclists. *Intl J. Sports Med.* **26**, 739–746.

Earnest, C.P., Foster, C., Hoyos, J., Muniesa, C.A., Santalla, A. & Lucia, A. 2009 Time trial exertion traits of cycling's grand tours. *Intl J. Sports Med.* **30**, 240–244.

Fallon, L. & Bell, A. 2005 *VIVA la VUELTA! 1935–2013*. Mousehold Press for Basque Children of '37.

Faria, E.W., Parker, D.L. & Faria, I.E. 2005*a* The science of cycling: factors affecting performance. Part 2. *Sports Med.* **35** (4), 313–337.

Faria, E.W., Parker, D.L. & Faria, I.E. 2005*b* The science of cycling: physiology and training. Part 1. *Sports Med.* **35** (4), 285–312.

Garcia-Lopez, J., Rodriguez-Marroyo, J.A., Juneau, C.E., Peleteiro, J., Martinez, A.C. & Villa, J.G. 2008 Reference values and improvement of aerodynamic drag in professional cyclists. *J. Sports Sci.* **26** (3), 277–286.

Gibertini, G. & Grassi, D. 2008 *Cycling Aerodynamics*, vol. 506. Springer.

Griffith, M.D., Crouch, T., Thompson, M.C., Burton, D., Sheridan, J. & Brown, N.A.T. 2014 Computational fluid dynamics study of the effect of leg position on cyclist aerodynamic drag. *Trans. ASME: J. Fluids Engng* **136**, 101105.

Hosoi, A.E. 2014 Drag kings: characterizing large-scale flows in cycling aerodynamics. *J. Fluid Mech.* **748**, 1–4.

Jeukendrup, A.E. & Martin, J. 2001 Improving cycling performance: how should we spend our time and money. *Sports Med.* **31** (7), 559–569.

Kyle, C.R. & Burke, E.R. 1984 Improving the racing bicycle. *Mech. Engng* **106** (9), 34–45.

Lucia, A., Earnest, C. & Arribas, C. 2003 The tour de france: a physiological review. *Scand. J. Med. Sci. Sports* **13**, 275–283.

Lucia, A., Hoyos, J. & Chicharro, J.L. 2001 Preferred pedalling cadence in professional cycling. *Med. Sci. Sport. Exer.* **33** (8), 1361–1366.

Lucia, A., Joyos, H. & Chicharro, J.L. 2000 Physiological response to professional road cycling: climbers vs. time trialists. *Intl J. Sports Med.* **21** (7), 505–512.

https://doi.org/10.1017/jfm.2020.1022 Published online by Cambridge University Press

MARTIN, J.C., MILLIKEN, D.L., COBB, J.E., MCFADDEN, K.L. & COGGAN, A.R. 1998 Validation of a mathematical model for road cycling power. *J. Appl. Biomech.* **14**, 276–291.

MCGANN, B. & MCGANN, C. 2012 *The Story of the Giro d'Italia. A Year-By-Year History of the Tour of Italy*. McGann Publishing.

MCGANN, C. & MCGANN, B. 2008 *The Story of the Tour de France*. Dog Ear Publishing.

MENASPA, P. 2015 Analysis of road sprint cycling performance. PhD thesis, Edith Cowan University.

MENASPA, P., ABBISS, C.R. & MARTIN, D.T. 2013 Performance analysis of a world-class sprinter during cycling grand tours. *Intl J. Sport. Physiol.* **8**, 336–340.

MENASPA, P., QUOD, M., MARTIN, D.T., ABBISS, C.R. & PEIFFER, J.J. 2015 Physical demands of sprinting in professional road cycling. *Intl J. Sports Med.* **36** (13), 1058–1062.

MIGNOT, J.F. 2016 *The Economics of Professional Road Cycling. Sports Economics, Management and Policy*, vol. 11. Springer.

MORTON, R.H. & HODGSON, D.J. 1996 The relationship between power output and endurance: a brief review. *Eur. J. Appl. Physiol.* **73**, 491–502.

PADILLA, S., MUJIKA, I., ANGULO, F. & GOIRIENA, J.J. 2000 Scientific approach to the 1-h cycling world record: a case study. *J. Appl. Physiol.* **89** (4), 1522–1527.

PADILLA, S., MUJIKA, I., CUESTA, G. & GOIRIENA, J.J. 1999 Level ground and uphill cycling ability in professional road cycling. *Med. Sci. Sport. Exer.* **31** (6), 878–885.

PADILLA, S., MUJITA, I., ORBANANOS, J., SANTISTEBAN, J., ANGULO, F. & GOIRIENA, J.J. 2001 Exercise intensity and load during mass-start stage races in professional road cycling. *Med. Sci. Sport. Exer.* **33** (5), 796–802.

PINOT, J. & GRAPPE, F. 2014 A six-year monitoring case study of a top-10 cycling grand tour finisher. *J. Sports Sci.* **33** (9), 907–914.

DI PRAMPERO, P.E., CORTILI, G., MOGNONI, P. & SAIBENE, F. 1979 Equation of motion of a cyclist. *J. Appl. Physiol. Respir. Environ. Exerc. Physiol.* **47** (1), 201–206.

SANDERS, D. & HEIJBOER, M. 2018 The anaerobic power reserve and its applicability in professional road cycling. *J. Sports Sci.* **37** (6), 621–629.

SANDERS, D. & HEIJBOER, M. 2019 Physical demands and power profile of different stage types within a cycling grand tour. *Eur. J. Sport Sci.* **19** (6), 736–744.

SANTALLA, A., EARNEST, C.P., MARROYO, J.A. & LUCIA, A. 2012 The tour de france: an updated physiological review. *Intl J. Sport. Physiol.* **7**, 200–209.

SOULA, D. 2013 *Passion maillot vert : le maillot vert de A à Z*. Cherche Midi.

UNDERWOOD, L., SCHUMACHER, J., BURETTE-POMMAY, J. & JERMY, M. 2011 Aerodynamic drag and biomechanical power of a track cyclist as a function of shoulder and torso angles. *Sports Engng* **14**, 147–154.

VAYER, A. & PORTOLEAU, F. 2001 *Pouvez-vous gagner le tour*? Polar.

VOGT, S., ROECKER, K., SCHUMACHER, Y.O., POTTGIESSER, T., DICKHUTH, H.H., SCHMID, A. & HEINRICH, L. 2008 Cadence-power-relationship during decisive mountain ascents at the Tour de France. *Intl J. Sports Med.* **29**, 244–250.

VOGT, S., SCHUMACHER, Y.O., ROECKER, K., DICKHUTH, H.-H., SCHOBERER, U., SCHMID, A. & HEINRICH, L. 2007 Power output during the tour de france. *Intl J. Sports Med.* **28**, 756–761.

WILSON, D.G. & SCHMIDT, T. 2020 *Bicycling Science*, 4th edn. MIT Press.

https://doi.org/10.1017/jfm.2020.1022 Published online by Cambridge University Press